

University of Louisville

## ThinkIR: The University of Louisville's Institutional Repository

---

College of Arts & Sciences Senior Honors  
Theses

College of Arts & Sciences

---

3-2024

### Impact of sodium benzoate and a high fat diet on kidney of mice.

Anna Lipinski

Follow this and additional works at: <https://ir.library.louisville.edu/honors>



Part of the [Biology Commons](#)

---

#### Recommended Citation

Lipinski, Anna, "Impact of sodium benzoate and a high fat diet on kidney of mice." (2024). *College of Arts & Sciences Senior Honors Theses*. Paper 316.

Retrieved from <https://ir.library.louisville.edu/honors/316>

This Senior Honors Thesis is brought to you for free and open access by the College of Arts & Sciences at ThinkIR: The University of Louisville's Institutional Repository. It has been accepted for inclusion in College of Arts & Sciences Senior Honors Theses by an authorized administrator of ThinkIR: The University of Louisville's Institutional Repository. This title appears here courtesy of the author, who has retained all other copyrights. For more information, please contact [thinkir@louisville.edu](mailto:thinkir@louisville.edu).

Impact of sodium benzoate and a high fat diet on kidney of mice

By

Anna Lipinski

Submitted in partial fulfillment of the requirements for

Graduation *magna cum laude*

And

for Graduation with Honors from the Department of Biology

University of Louisville

March 2024

## INTRODUCTION

Throughout the course of history, the availability of “safe foods” for consumption was limited due to lack of compounds proven to extend shelf life. Spoilage was a prominent universal issue, with bacterial and microorganism activity rendering food unsafe for consumption (Centers for Disease Control [CDC], 1999 /48(40);905-913). During storage microbial agents quickly inhabit food. Conditions which make inhabitation more favorable for bacteria and other microorganisms include warm temperatures, moisture, and open air environments (Odeyemi et al. 2020). Due to the quick nature of microorganism reproduction, food spoilage becomes unavoidable after a short period of time. Consequently, the addition of both natural and synthetic chemical compounds in food became more prominent in the mid-twentieth century (Jackson 2009), to extend product shelf life significantly and resist quick spoilage.

Sodium benzoate (SB) became an attractive compound to serve as a food preservative due to its tasteless properties, excellent solubility, and ability to inhibit bacterial and fungal growth in storage conditions (Davidson et al. 2005). The mechanism by which this occurs begins upon benzoic acid absorption into the cells of microorganisms which, at pH of 5 or less, inhibits anaerobic fermentation of glucose. This decreases the available stores of nutrients, thus inhibiting the growth and survival of microorganisms responsible for food spoilage (Pongsavee 2015). The natural form, benzoic acid, consists of a benzene ring with a carboxyl group substituent (Sim et al. 1955), and it is found in numerous spices (such as cinnamon) and plants (most commonly among berries such as blueberries and cranberries). However, reacting benzoic acid with sodium hydroxide yields the synthetic form incorporated into foods, beverages, and everyday products to increase shelf life. Inclusion of SB into products is intended to limit bacterial growth and food spoilage, which is optimized in foods with acidic pH values and

carbonated products. More specifically, fruit juices, fermented compounds (beer, yogurts, canned vegetables), and processed foods are common products which utilize sodium benzoate (Shahmohammadi et al. 2016). However, in recent decades there is an increasing exposure to SB stemming from consumption of carbonated drinks such as soda and fruit juices, as well as sauces and condiments (Tfouni & Toldeo 2002). Studies conducted following daily diets in the United States found that daily consumption of ultra-processed foods high in preservatives grew from 53.5 percent to 57 percent of daily calories between 2001 to 2018 (Juul et al. 2022). Exposure to SB has also increased through other routes—as SB is included in moisturizers, hand soap, shampoo, and more (Ikarashi et al. 2010). Therefore, the increase in exposure to SB is the result not only from shifts in daily diets, but also from its inclusion into a wide variety of other daily products.

Metabolism of SB occurs in mitochondria through a two-step mechanism (Badenhorst et al. 2014). In the mitochondrion, it is quickly converted to benzyl-CoA in the mitochondrial matrix through consumption of ATP and glycine. The next step requires the enzyme glycine-N-transferase, which mediates the transformation of benzoyl-CoA to hippurate. Therefore, increasing consumption of foods including sodium benzoate is closely linked to increases in levels of serum benzoate and hippurate (Kubota 1991). Benzoate absorbed by the gastrointestinal tract is metabolized in the liver to hippurate, which is then excreted from the body in urine produced by the kidneys (Chen et al. 2009).

In the late twentieth century, the use of SB as a food preservative was evaluated by the Food and Drug Administration (FDA) (Code of Federal Regulations, Title 21). Initial FDA regulations in 1977 on manufacturing companies would permit use of SB as a food preservative at maximum limits of 0.1% by weight or volume. Under this limit, the FDA further granted SB

generally regarded as safe (GRAS) status. Further evaluation of the compound by the Joint Food and Agriculture Organization of the United Nations and the World Health Organization (WHO) Expert Committee on Food Additives in 1996 recommended a daily limit of consumption at doses 0-5 mg/kg of body weight, and this was increased to 0-20 mg/kg of body weight in 2021 (JECFA 1996 and 2021).

While a number of studies in animals have reported effects of SB in kidneys, the gap in knowledge is determining SB effect on kidneys in the setting of obesity. This is important due to the prevalence of obesity and metabolic disorders and their known impact on kidney disease. The goal of the current study was to determine the effects of SB on kidneys of both male and female mice in combination with consumption of a high fat diet, as an established model of obesity, metabolic syndrome and chronic kidney disease. Reports suggest altered kidney function and increased oxidative stress in kidneys of mice treated with SB. However, the effects of dietary SB exposure on specific renal structures are unclear. Therefore, this study addressed the hypothesis that SB with a high fat diet will increase extracellular matrix production and alter anti-oxidative regulators and enzymes in kidneys of female and male mice.

## **LITERATURE REVIEW**

In addition to its use as a preservative, SB is also used for therapeutic purposes in managing symptoms of anxiety, depression, and other neurodevelopmental disorders, as well as for treatment of encephalopathy. From a clinical stance, specific and regulated dosages of SB have been correlated with an anti-inflammatory response promoting the management of a diverse selection of psychiatric disorders. Acting as a D-amino acid oxidase DAAO inhibitor, SB regulates the stimulation of NMDA receptors, crucial components of the brain's communication system, and control of neurotransmission. Downregulation of these specific receptors contribute

to onset of schizophrenia (MacKay et al. 2019), while increased stimulation has been linked with the progression of Alzheimer's disease (AD) and dementia. In a study with SB for treatment of chronic schizophrenia, patients were followed over a twelve-week period, administering 1000 mg/day SB (equivalent to around 15mg/kg/day based on average patient weight around 68kg) in combination with active therapy treatment. Following completion of the trial, those in combination therapy were shown to have significantly decreased scores on the Positive and Negative Syndrome Scale (PANSS) by 20% –as determined by an increase in cognitive processing speed, pattern recognition, and overall improvement of neurocognition, compared to control groups with placebo pills in combination with therapy showing only a 4-10% reduction in PANSS scores (Lane et al. 2013). In animal models, single dose oral treatments with SB (100, 300, or 1000 mg/kg b.w.) reduced impulsive deficits and hyperlocomotion (Matsuura et al. 2015). Another study examined effects of SB for treatment of AD, in which patients with mild cognitive impairments secondary to AD were administered 250-750 mg/day of SB (equivalent to 3.5-11mg/kg/day, considering average body weight of 70kg) over a 24-week period, to observe changes in cognitive skills. Results showed improvement of both memory retention and verbal learning skills –likely due to SB's ability to regulate NMDA receptors in the CNS (Lin et al. 2014).

Another therapeutic use with SB is treatment of hepatic encephalopathy (HE), characterized by a decline in cognitive function, compromised neuromuscular activity, altered consciousness, sleep disorders, and overall mood shifts (Misel et al. 2013). Largely due to elevated blood ammonia levels, HE onset leads to several direct and indirect symptoms. The increased levels of ammonia in the blood are the result of multiple complications, with decreased elimination secondary to liver cirrhosis exacerbated by increased kidney production of ammonia

due to metabolic alkalosis being the two largest contributing factors. SB was implemented in HE treatment since at least 1979 due to its ability to excrete ammonia through a urea cycle independent pathway (Misel et al. 2013). To test this, one study administered 5 g oral SB twice daily to 36 patients with liver cirrhosis or portosystemic anastomosis and HE for less than 7 days duration. Following treatment for  $11.6 \pm 6.4$  days, 80% of patients (30 patients) receiving SB recovered – determined based on normalization of blood ammonia levels in 94% (34 patients) and improvement of general mental status in 79% (30 patients) (Sushma et al. 1992).

As SB became more prominent in use as a food preservative and in other products, so have concerns for increasing and chronic exposure to SB (Piper et al. 2017). A concern with SB is the potential for altered chemistry when in combination with other additives and chemicals. In combination with ascorbic acid (vitamin C), another common additive, and metals, benzoate salts can be converted to benzene, a known carcinogen. Benzene can be formed through decarboxylation of benzoate by hydroxyl radicals generated through metal-catalyzed reduction of  $O_2$  and  $H_2O_2$  by ascorbic acid, in a process driven by heat, conditions common during food/product manufacturing processes and storage conditions (Gardner et al. 1993). Furthermore, comparison of foods with and without addition of benzoates found benzene at levels ranging from 1-38ng/g and  $<2$ ng/g, respectively. (McNeal et al. 1993). Other causes for concern with SB include effects on tissues and cells. For example, SB increases release of histamine and prostaglandins from gastric mucosa and these factors may play a role in modulation of allergic reactions or other immune regulatory pathways (Schaubschläger et al. 1991). The metabolic effects of SB exposure on regulation of blood glucose has also been examined, since studies have shown benzoates and hippurate have negative effects on glucose and insulin homeostasis. Metabolism of SB metabolism in the mitochondria can increase ATP and glycine utilization and

sequester coenzyme A, and thus lead to metabolic effects (de Vries et al. 1948). In addition, hippurate increased in blood following exposure to SB, and hippurate leads to impaired glucose uptake in cultured cells and utilization by muscle (Spustova & Dzurik 1991, Spustová et al., 1987). In one study, sheep were injected intravenously with 39-1250  $\mu\text{mol/kg}$  benzoic acid. Both insulin and glucagon secretion increased dose dependent manner (Mineo et al. 1995) with benzoic acid, as well as with benzoic acid derivatives, indicating that benzoic acid and derivatives (ie, SB) may shift glucose homeostasis away from equilibrium. However, Lennerz et al (2015) compared the blood glucose levels of 14 overweight patients following a single oral dose of 0.1% SB in a 75 g glucose solution, finding minimal nonsignificant elevation in comparison to controls not receiving SB. While the administered dose in this trial fell within the GRAS FDA recommended level, the effects of chronic exposure to SB on blood glucose homeostasis in humans remains to be defined.

The effects of SB on body weight and multiple organ systems have been examined in multiple animal studies. One study follows a 4-8 week exposure period for male rats to oral sodium benzoate at doses of 2-5% concentrations. It was concluded that those with 2% SB exposure showed no obvious adverse effects or significant weight changes; however rats exposed to 5% SB were noted to have severe weight reductions (Informatics, Inc 1972). Additional studies conducted in 1993 uphold these findings: both F344/N rats and B6C3F mice were exposed to 1.8-3% SB doses for 10 consecutive days. Results showed both female and male rats exposed to higher concentrations of SB had reduced body weight, increased liver and kidney mass, and increased protein accumulation. Additional findings in mice showed significant increases in female kidney mass and male liver mass (Fujitani et al. 1993). Through additional



studies assessing SB exposure at different concentrations, it was proven that lower doses of  $\leq 2\%$  showed the lowest risk to adverse effects when compared alongside increasing doses.

A number of studies in animals have reported effects of SB in kidneys. This is important as the kidneys play an important role in excretion of hippurate, the product of SB metabolism. The kidneys filter blood to remove wastes and excrete them from the body through urine and thus are a vital component to maintaining homeostasis in the body, more specifically through the role in osmoregulation –the balancing of fluid filtration and reabsorption and secretion of ions, and regulation of blood pressure. Each kidney is subdivided into a cortex and medulla, representing the outer layer and inner layer, respectively (Widmaier et al. 2023). The functional unit of the kidney is the nephron, composed of a glomerular capillary bundle, which is the filtering unit of the kidney and surrounded by a Bowman’s capsule, as well as a network of tubules with specialized cell types with differing functions. Blood enters the glomerulus from the afferent arteriole and the high hydrostatic pressure in the glomerulus allows blood to be filtered through the fenestrated endothelial cells lining the glomerular capillary and the filtration barrier, composed of the basement membrane and slit diaphragm formed by foot processes of specialized epithelial cells (podocytes) that reside on the outer surface of the capillaries. Blood cells and most blood proteins do not pass through the filtration barrier, and are retained within the glomerular capillaries before exit through the glomerulus via the efferent arteriole for return to general circulation. The filtrate, or filtered blood, moves from the Bowman’s space of the glomerulus into a complex network of tubules. The first site encountered in this network is the proximal convoluted tubule (PCT), where nearly 70% of minerals such as sodium, amino acids and 100% of glucose in the filtrate will be reabsorbed for entry into the peritubular capillaries and return to systemic circulation. (Horita et al. 2017). However, it is to be noted that secretion

also occurs in this site, with the nephron pulling waste products such as hydrogen ions, potassium ions, and ammonia for excretion into urine. The apical (filtrate or urine side) and basolateral (blood side) membranes of the PCT contains several different transporters specific for ion passage, with some active transporters and others co-transporters that exchange ions being reabsorbed from or secreted into the filtrate (eg, sodium/hydrogen exchanger & sodium/glucose exchanger) (Horita et al. 2017). Filtrate from the PCT then enters the descending loop of Henle, which extends deep into the medulla cortex, followed by the ascending loop of Henle in the opposite direction. Due to selective permeabilities in each portion, these segments are responsible for reabsorption of water and salts in a process named the countercurrent system (Dantzler et al. 2013).

Next, the filtrate enters the distal convoluted tubule (DCT) where some secretion of waste products still occurs (Castaneda-Bueno et al. 2022). Macula densa cells within the DCT are highly involved in regulation of glomerular filtration rate (GFR) and regulation of blood pressure in response to the hormone aldosterone, secreted when blood pressure decreases (Widmaier et al. 2023). The final structure filtrate enters prior to excretion is the collecting duct, where cells also respond to antidiuretic hormone (ADH) for insertion of aquaporin-2 transporters (AQP2) into the apical membrane of collecting duct cells (Ranieri et al. 2019), to increase reabsorption of water across the membrane to return to the blood and restore homeostasis.

Kidney injury in response to drugs, diet, obesity, and metabolic disorders such as diabetes, and other environmental or genetic factors will eventually lead to decreased kidney function and progression to chronic kidney disease (CKD). Diagnosis of CKD requires a minimum of three consecutive months of reduced kidney function, as defined by reduced GFR ( $<60$  mL/min), increased albumin excretion ( $\geq 30$  mg/day), abnormal urine sedimentation or

histological changes, or tubular alterations (Chen 2020). Recent trends following the incidence of CKD from the United States Renal Data System (United States Renal Data System [USRDS] 2023) have shown CKD prevalence among populations under 65 years old has increased from 7.7 percent in 2007 to 9.0 percent in 2020 (USRDS 2023). Another interesting finding is the correlation between obesity and CKD incidence. While the general population incidence of obesity increased from 32.5 percent in 2005 to 40.7 in 2020, it was also found that the incidence of obese individuals with CKD increased from 42.4 percent in 2005 to 50.2 percent in 2020 (United States Renal Data System [USRDS] 2023). Studies evaluating histological changes in kidneys of obese individuals have found increased incidence of glomerular hypertrophy (Kambham et al. 2001), increased proteinuria, tubular hypertrophy, interstitial inflammation, and fibrosis resulting from increased production of extracellular matrix proteins (Decleves et al. 2014). Histological changes observed in cases of obesity may contribute to onset of CKD through impairment of filtration and excretion of waste products. Alterations in the interstitium and increased inflammation in the kidneys may further link changes in extracellular matrix composition to daily diet choices.

Since the turn of the twenty-first century, there has remained an increase in the incidence of obesity and obesity-related health conditions (Stierman et al. 2021). While some contributing factors for obesity are genetically predisposed, the roles of excess caloric consumption and high fat diets have become of increasing concern. A well-balanced and nutrient-dense diet has become an economic burden in some countries, such as the United States, where the prevalence of obesity has increased from 30.5-41.9% from 1999-2020 (Stierman et al. 2021). With obesity comes a strong predisposition for several kidney diseases, with diabetes mellitus (DM), hypertension (HTN), and chronic kidney disease (CKD) among the most prevalent. Therefore,

the role of a high fat diet in relation to onset of kidney disease is of increasing interest to understand.

A prior study assessed effects of high fat diet (HFD) consumption in male mice on markers of inflammation and found that obese mice with a HFD exhibited an increase in the pro-inflammatory markers interleukin (IL)-6 and tumor necrosis factor- $\alpha$  and a reduction in IL-10, (Sanchez-Navarro et al., 2021) an important anti-inflammatory protein. In addition, HFD led to significant reduction in FOXO3 protein levels in contrast to healthy controls. FOX3 protein is a critical part in the defense against oxidative stress associated with CKD, thus a reduction correlates with increased inflammation observed in reports. Furthermore, obese mice had glomerular hypertrophy, and while overall renal fibrosis was not elevated as measured by picrosirius red staining of extracellular collagen fibers for this duration of HFD consumption, transforming growth factor beta mRNA was significantly increased, indicating activation of pro-fibrotic signaling pathways. Another study with male mice on HFD also reported an increase in albumin excretion, glomerular size and glomerular mesangial matrix, as well as deposition of type IV collagen in kidneys, an extracellular matrix protein increased in CKD associated with diabetes and kidney fibrosis (Deji et al., 2009). Additional studies conducted on both mice and rats demonstrate that a HFD induces oxidative stress in the kidneys through accumulation of ROS and inflammatory cytokines (Sun et al. 2020) (Ha et al. 2022). The effects of a combination of HFD and SB on kidneys remains to be defined

Maintaining a balance of the extracellular matrix (ECM) is essential in preserving its function. The ECM is composed of various glycoproteins, collagens, elastins, and proteoglycans that contribute to formation of basement membranes and interstitial space for overall organ stability (Bulow & Boor 2019). Specific components of the interstitial ECM include collagens

(types I, III, IV, V, VI, VII, and VIII) and glycoproteins (e.g., fibronectin, laminin), which can be used as markers for assessing function and structural changes of the kidney. Therefore, measuring ECM protein content over time may provide insight into kidney disease onset and further progression of the condition. The ECM of healthy kidneys exist in a state of equilibrium, actively undergoing remodeling through recycling and replacement of aged or damaged proteins. However, disruptions in this balance may induce histological changes associated with fibrosis and an onset of kidney disease. Renal fibrosis has a complex morphology, and it may manifest in diverse outcomes and structural changes depending on other contributing factors. Nevertheless, accumulation of ECM proteins remains a predominant biomarker of the progression of renal fibrosis (Bulow & Boor 2019). Thus, the upregulation of collagen production and induction of pro-inflammatory pathways are significant contributors to the onset of fibrosis. Furthermore, elevated ECM protein deposition is a closely linked morphological change observed in cases of chronic kidney disease (CKD), which may manifest into end-stage renal disease (ESRD) due to impaired filtering secondary to fibrosis. Through use of picro-sirius red stains or immunohistochemistry of specific proteins, the degree of fibrosis can be quantified as a measure of risk for disease onset or further disease progression. Specific regulation of ECM components in kidneys following exposure to SB remain to be examined.

Many studies on the effect of SB on kidneys have analyzed markers of oxidative stress-related mechanisms. Reactive oxygen species (ROS) are important for normal cell biology. Cell redox status is maintained by the balance between generation and detoxification of ROS. Oxidative stress results from increased production and decreased degradation of ROS. Therefore, intact functioning of cell anti-oxidative defense mechanisms are critical. There are multiple species of ROS such as superoxide, hydroxyl radical, hydrogen peroxide, and peroxynitrite,

which can react with and alter function of cell proteins, carbohydrates, and phospholipids. Increases in ROS can degrade components of the basement membrane (Thakur et al. 1988). Therefore, it has been of increasing interest to study oxidative and inflammatory markers in response to SB within the kidneys, which may provide an understanding of how kidney function and structure may be altered following exposure. However, SB also exhibits properties as a hydroxyl radical scavenger, protecting the cell from damage induced by free radicals and oxidative stress. Several studies have explored this property of SB to potentially attenuate kidney injury in animals in response to nephrotoxic agents. Thakur et al (1988) used Sprague-Dawley rats injected with puromycin aminonucleoside (PAN) to induce nephrotic syndrome, a disorder characterized by excess proteinuria. SB (150 mg/kg) was then injected intraperitoneally twice daily for seven days. Although PAN increased proteinuria, this was significantly ( $p < 0.05$ ) reduced in rats treated with SB, thus indicating that SB may have a therapeutic use in treatment of proteinuria. Similarly, SB was shown to improve kidney function and histology in response to gentamicin (Walker & Shah 1983), glycerol-induced (Shah and Walker 1988) kidney injury, and reduced proteinuria in passive Heymann nephritis model of kidney injury (Shah 1988) in rats. Alternatively, SB did not improve proteinuria in response to doxorubicin hydrochloride kidney injury (Milner 1991).

Other studies evaluated the role of SB as a D-amino acid oxidases (DAAO) inhibitor, which is responsible for the oxidation of D-serine with production of ammonia and hydrogen peroxide byproducts. In kidneys, high doses of D-serine has been shown to induce necrosis of the proximal renal tubules (Ganote et al. 1974). Necrosis describes damage to tubular cells involved in secretion and reabsorption, causing decreased filtration of toxins and onset of kidney disease if not reversed. In one study, rats were first administered a one-time dose of saline or of

SB (125, 250, 500, 750 mg/kg) intraperitoneally, and one hour later given either D-serine (dose 500 mg/kg) or deionized water. Histological analysis showed reduced severity of tubular necrosis in rats pretreated with SB. D-serine treated rats showed increases in urine glucose and protein, suggesting tubular damage compromising filtration, and SB decreased urine glucose and protein levels (Williams and Lock 2005). While this may indicate SB holds a protective effect against necrosis, this study tested only one-time doses of SB. In a separate study, the protective effect of SB in response to 2,8-dihydroxyadenine crystal-induced model of chronic kidney disease, was not dependent on DAAO inhibition, as DAAO-deficient mice treated with SB still showed protection from kidney injury (Oshima et al. 2023).

Additional studies in animals more closely examined the solitary effects of SB on kidneys. In one study, albino rats were administered 100 mg/kg SB in drinking water for 15 consecutive weeks. There was a significant increase in serum creatinine and urea in SB-treated rats in comparison to controls (Zeghib & Boutlelis 2021). Creatinine is a byproduct of creatine metabolism in the muscles and a widely utilized marker for glomerular filtration rate (GFR) and thus overall kidney function. Because it is freely filtered and not reabsorbed (Traynor et al. 2006), increases in serum creatinine indicates decreased filtration at the glomerulus. Urea is the byproduct of ammonia metabolism in the liver, and is another marker used in analyzing kidney function. Although about 40-50% of urea is reabsorbed in the proximal tubule, increases in serum urea beyond the normal level also indicate reduced glomerular filtration (Traynor et al. 2006). Thus, the increases in serum creatinine and urea observed in this study following 15-week SB administration indicates significant kidney function impairment. Histological changes, while reported, were not clearly shown and remain to be determined. Thus, while a single dose of SB

may act to protect against D-serine induced necrosis, long-term SB exposure appears to actually induce tubular necrosis.

In another similar study, work conducted at Cairo University examined tubular epithelial cells of 60 male albino rats following administration by oral gavage of 0.9 mg/kg b. wt. for 90 days. Histological changes observed in SB treated rats were significant for tubule and epithelial cell degradation as well as leukocyte infiltration (Abd-Elhakim, Y. M. et al 2023). The destruction of tubule and epithelial layers indicates SB may contribute to loss of structural integrity of the kidney. Additional findings were significant for thickened basement membranes and glomerular edema (Abd-Elhakim, Y. M. et al. 2023) further supporting prior evidence that SB has a damaging effect on kidney structure. Furthermore, the antioxidative enzymes superoxide dismutase and catalase, as well as an ROS detoxifier and anti-oxidative enzyme co-factor, glutathione (GSH) were decreased, while MDA (malondialdehyde), a marker of lipid peroxidation and thus oxidative stress, was increased in kidneys. A study by Yassein et al (2022) in which male rats received SB 200mg/kg, orally, for only 6 weeks, also found decreased SOD activity and increased MDA content in kidneys. In another study of male mice that were fed a standard diet with either 0, 125, 250, or 500 mg/kg SB for 8 weeks, serum SOD activity significantly increased with 125 and 250 mg/kg SB, but decreased at a dosage of 500 mg/kg (Olofinnade et al. 2021). This suggests a SB diet promotes elevated oxidative stress, as indicated by the increased response of SOD to neutralize free radicals; however, as dosage increases to 500 mg/kg b. wt. SOD levels decrease below control levels indicating impaired response to ROS.

## **METHODS AND PROCEDURES**

### **Experimental mouse model**



All mouse studies were conducted in accordance with approved IACUC protocols. Mice were kept in clean housing with 12h light/dark cycle and unlimited access to food and water in an Association for Assessment and Accreditation of Laboratory Animal Care-accredited facility. Five week-old C57BIL/6J male (n=20) and female (n=20) mice were randomly assigned to either a control diet (CD) or a high fat diet (HFD, 21% fat) for 6 weeks, then received sodium benzoate (SB; 99mg/kg) or sterile water, by gavage, for 4 additional weeks. Therefore, there were 3 factors (diet, SB, sex) producing 8 experimental groups. The diets were composed by weight of the following nutrients: Control diet (Teklad TD.08485, Inotiv; West Lafayette, IN), 17.3% protein, 61.3% carbohydrate, and 5.2% fat; High fat diet (Teklad TD.88137, Inotiv), 17.3% protein, 48.5% carbohydrate, and 21% fat. Body and kidney weight were measured on the date of mouse euthanization.

### **Kidney Tissue preparations**

Half of one kidney was fixed in formalin for 24h, then transferred to 70% ethanol for processing and paraffin embedding. These samples were used for preparation of kidney sections on slides and histologic staining and analysis. The remainder of the kidney material was divided, snap frozen in liquid nitrogen and stored at -80°C. Frozen kidney pieces were homogenized for protein extraction/western blotting (see below).

### **Picro-sirius red staining of kidney sections:**

Picro-sirius red stain was used to determine the presence of collagen fibers in the interstitium of the kidneys. Formalin-fixed paraffin-embedded kidney sections (4µm) prepared on glass slides were de-paraffinized in 3 changes of xylene (5min each) and rehydrated in graded

ethanols (100%, 95% , 70% ethanol; 5 min each), followed by water. Sections were incubated in picro-Sirius red stain solution (Abcam; Waltham, MA) in a humidified chamber for 1h, followed by quick rinses in 0.5% acetic acid. Sections were then dehydrated in 100% ethanol (2x, 30s), cleared with in xylene (2x, 30s), and coverslips added using Vectamount mounting medium (Vector Labs, Newark, CA).

### **Analysis of picro-sirius red staining:**

Images of picro-sirius red-stained samples were captured with an Olympus BX51 light microscope coupled to a Q-color 5 camera, Image-Pro 6.2 software (Media Cybernetics, Silver Spring, MD) using a 20X objective. Around 20 photos of kidney cortex were captured from each section using the same exposure time and color saturation settings. Seven to ten of the images/section without tissue overlap were selected for blinded image analysis with Image-Pro software and calibrated for 20X magnification. Specific sirius red staining representative of extracellular collagen fibers were selected in a color profile. Non-specific staining, such as nuclear or cell cytoplasmic staining, was excluded from selection. The sum of the area of detected pixels was measured and the surface area of tissue included for picro-sirius red stain selection manually outlined for measurement, since many images included areas devoid of tissue or areas within tissue not suitable for analysis, such as folding of the tissue section. The ratio of the sum of detected area to tissue surface area of each image was calculated, as previously described (Merchant et al 2020).

### **Homogenization of kidneys for protein extraction:**

Proteins were extracted from kidneys for utilization in western blotting procedures (see below). Frozen pieces of whole kidney were homogenized on ice in 1.5ml micro-centrifuge tubes in 250µl ice cold lysis buffer containing 10% glycerol, 50mM HEPES, 100mM KCL, 2mM EDTA, 0.1% NP40, 10mM NaF, 0.25mM NaVO<sub>3</sub>, 1X HALTS protease inhibitor). Tissues were disrupted by grinding and twisting with a pestle tool specific to the tube size, until no visible tissue clumps remained, and left on ice for 10 minutes. Next, each sample was passed through a 21-gauge needle over ice 10 times to further disrupt extracts, and left on ice for 5 minutes. Samples were then transferred to a bath sonicator for 2 minutes, then transferred back to ice bath for an additional 5 minutes. Each sample was then run through a 200µl pipette 10 times followed by centrifugation for 30 minutes at 4 °C and 13,000 RCF. Cleared extracts were transferred to a clean and stored at -80°C. To prepare for protein assay, cleared samples were diluted 1:20 in lysis buffer and protein concentration in each assay measured using Bio-Rad Protein Assay buffer (Bradford assay; Bio-Rad; Hercules, CA), using the micro-assay procedure for microtiter plates.

### **Western Blot:**

A western blot is used to detect the abundance of a specific protein by using an antibody against the protein. Ten micrograms of protein extract from each mouse was used for western blotting to analyze abundance of specific proteins. Extracts from 3 different mice in each of the 8 experimental mouse groups were analyzed and each western blot included one sample from each of the 8 mouse groups. Extracts were prepared for western blotting by reduction of disulfide bonds with DTT (dithiothreitol; 50mM) and NuPage LDS-sample buffer (141 mM Tris base, 106 mM Tris HCl, 2% LDS, 10% Glycerol, 0.51 mM EDTA, 0.22 mM SERVA Blue G, 0.175 mM

Phenol Red, pH 8.5; Invitrogen), and heating at 99°C for 5min. Protein were separated based on size by electrophoresis using pre-cast Bis-Tris gels (4-12%, 1mm; Invitrogen; Carlsbad, CA) and MES running buffer (Invitrogen) at 200V for 40 min, then transferred to nitrocellulose membrane (0.45µm) at 30V for 60min. Following protein transfer, membranes were stained with Ponceau-S protein stain to confirm protein transfer and ensure lack of bubbles that may have hindered protein transfer in molecular weight range of the target proteins to be analyzed. Next, membranes were blocked with 5% nonfat (NF) milk /TTBS (Tris-buffered saline) for 30 minutes at room temperature, followed by overnight incubation at 4°C in the following primary antibodies prepared in 5% BSA(bovine serum albumin)/TTBS: rabbit anti-fibronectin (Sigma cat. No. #F3648, 1:1000); rabbit anti-γ-GCSc (Glutamyl-Cysteine Synthetase/catalytic subunit; Santa Cruz cat. No. #22755, 1:500); rabbit anti-SOD-1 (Superoxide dismutase-1; Santa Cruz cat. No. #11407, 1:2000); mouse anti-GAPDH (Glyceraldehyde phosphate dehydrogenase; Millipore; 1:150,000). The next day membranes were washed 3 x 5 minute in TTBS and incubated in respective horse radish peroxidase-conjugated, goat-anti-rabbit or goat-anti-mouse secondary antibody (Cell Signaling [Danvers, MA] cat. #7074, 7076; 1:2000 in 5% NF milk/TTBS) for 1 hour at room temperature. Following three 5 minute washes with TTBS, membranes were incubated with peroxide/luminol chemiluminescent substrate (Pierce/ Thermo scientific; Waltham, MA) for 1 minute. Chemiluminescent light emission from protein band/antibody complexes were captured with a Bio-Rad Imager coupled to Image Lab software. To quantify abundance of specific proteins, densitometry of western blot bands was conducted using ImageJ software, available from the NIH (imagej.net). Western blotting of GAPDH was conducted to serve as a measure of total protein loading in each lane. GAPDH is often used as a housekeeping protein with steady expression (Nie, W et al 2017). Thus, the ratio of densitometry

values for SOD-1, GCSs, and FN in each lane to GAPDH was used to normalize abundance of each protein to protein loaded in each lane.

### **Data presentation and Statistical Analysis**

Bar graphs are mean  $\pm$  SD or SEM, as specified in figure legends. Comparison of experimental outcomes (body weight, relative kidney weight, western blot data, picro-sirius red staining) between experimental mouse groups was performed using a 3-way ANOVA with full model (linear + interactions), followed by multiple comparisons using Tukey's test (HSD - honestly significant difference), in Matlab 2023b (The Mathworks). P-values  $<0.05$  were considered statistically significant.

## **RESULTS**

### **Effects of HFD and SB on mouse body weight and the ratio of kidney weight to body weight**

Previous reports on effects of SB in rats have shown a decrease in body weight, while mice were found to have increased body weight (Fujitani 1993). In the current study, mouse body weight for each group was measured following completion of the 10 weeks of the experimental duration. Based on 3-way ANOVA there was a significant effect of sex ( $p < 0.01$ ) for increased body weights in males, compared to females (Figure 1). Multiple comparisons with Tukey post hoc analysis showed body weights in male mice in all groups were significantly increased compared to females in the same experimental groups. In addition, there was significance for an interaction between sex and diet ( $p < 0.01$ ), as males in the HFD group had higher body weights, compared to male mice on control diet and this effect was not altered by treatment with SB. In

addition, the 3-way ANOVA results showed a significant interaction between sex and SB treatment ( $p < 0.01$ ).

The ratio of kidney weights (both kidneys) to body weight was calculated and based on 3-way ANOVA analysis, diet had a significant ( $p < 0.01$ ) effect and there was a significant interaction between sex and diet (Figure 2). These results showed that in male mice the HFD group had significantly lower kidney weight/body weight ratios, and this effect was not altered by treatment with SB.

### **Effects of HFD and SB on extracellular matrix proteins**

Preliminary lab findings on kidneys sections of mice in this study showed HFD +/- SB treatment causing increased tubule vacuolization in male mice, compared to female mice. Picro-Sirius red histological staining solution stains collagen I and III fibers in the ECM, and is used to determine the extent of ECM expansion and/or fibrosis in kidney disease. Stained collagen fibers are indicated by dark red staining on stained tissue sections. Figure 3 shows representative picro-sirius red-stained kidney sections in female mice from all four diet and treatment groups. Similarly, Figure 4 shows representative images from male mice from all four groups. All images shown are from kidney cortex. Green arrows on images point to specific picro-sirius red-staining in the interstitial regions of kidney cortex and staining of these structures were selected by Image-Pro software for quantitation. Results of picro-sirius red staining analysis are shown in Figure 5. Based on a 3-way ANOVA, results show a significant effect of sex ( $p = 0.02$ ), with an overall increase in picro-sirius red staining in kidney cortex of female mice, compared to male mice (Figure 5). In addition, there was a significant interaction between diet and treatment ( $p = 0.02$ ). Post hoc analysis found a significant decrease in female mice on a high fat diet compared to female mice on a control diet.

The abundance of ECM proteins was also analyzed by western blot analysis of fibronectin in whole kidney protein extracts from each group. Fibronectin expression increases in kidney diseases such as diabetes that are associated with fibrosis. As shown in Figure 6, abundance of fibronectin was not different between any of the mouse groups, although the p-value for the effect of sex alone was 0.08, suggesting that fibronectin in males had a trend toward higher abundance, compared to female mice.

### **Effects of HFD and SB on protein abundance of enzymes in anti-oxidative defense pathways**

Abundance of enzymes in cellular antioxidative defenses were analyzed by western blot. Whole kidney protein extracts were analyzed for abundance of  $\gamma$ -glutamyl-cysteine Synthetase/catalytic subunit (GCS). This enzyme is responsible for the rate limiting step in synthesis of glutathione. As an antioxidative molecule, glutathione neutralizes ROS and can detoxify molecules. Furthermore, cycling of reduced and oxidized forms of glutathione plays an important role in maintaining cellular redox balance and activity of enzymes, such as glutathione peroxidase in catalysis of hydrogen peroxide. As shown in Figure 7, sex had a significant ( $p = 0.01$ ) effect on GCS with an overall decreased abundance in male mice, compared to female mice. Removing diet as a variable in the post hoc multiple comparisons analysis revealed a p-value of 0.06 between female and male mice in the water treatment groups, close to reaching significance.

Next, abundance of superoxide dismutase-1 (SOD-1) enzyme was analyzed in whole kidney protein extracts. This enzyme catalyzes the breakdown of superoxide radicals to molecular oxygen and hydrogen peroxide and plays a significant role in cell antioxidative defense mechanisms. Activity and/or abundance of SOD-1 has been shown to be both increased and decreased in animal models following exposure to SB, as well as in animal models of CKD.

As shown in Figure 8, as well as results of a 3-way ANOVA analysis, abundance of SOD-1 protein was not altered between any of the mouse groups.

## **DISCUSSION**

While SB is generally considered safe for consumption, some reports of treatment of animals within the GRAS limits of SB in humans show altered kidney function and/or markers of injury. With the prevalence of obesity and the reported effects of obesity and a consumption of a HFD on kidneys, the goal of this study was to determine the effects of SB in combination with a HFD, in male and female mice kidneys. The results of this study showed that SB did not alter the effect of HFD on body weight of male mice, and abundance of GCSc protein is significantly reduced in kidneys of male mice. These results suggest that male mice may be more susceptible to kidney injury in response to additional nephrotoxic conditions.

Similar to previous reports, males on a high fat diet had increased body weight. However, this effect was not altered with SB treatment. In addition, in contrast to prior reports (Fujitani 1993), SB alone did not alter body weight. This may be due to differences in mouse strain (C57Bl/6J vs B6C3F). This is different than results of female mice body weight, in which there was no significant difference following a high fat diet +/- SB. Similarly, due to increased body weight, the kidney to body weight ratio was only decreased in male mice, and SB had no additional effects to that of HFD.

Picro-Sirius red staining of kidney sections allowed for visualization and quantification of collagen fibers in the interstitium and a measure of ECM production. There was a significant difference in specific staining with picro-sirius red in female/CD/water mice compared to female/HFD/water mice. However, there were no significant differences reported in the remaining groups. The increased staining visualized in the female/CD/water group is likely a



limited finding due to several factors. First, one female mouse in the CD/Water group had increased tubular damage based on previous histological analysis. This is likely due to possible undetected illness of the mouse during the experimental trial. Also, there was significantly increased nonspecific staining from picro-sirius red in kidney sections from all mouse groups including non-matrix regions, and cell nuclei that also stained red. This affected analyzing the images in ImagePro, which was unable to differentially apply the color profile created for specific staining selection, leading to omission of specific staining in numerous cases. In combination, all of these limitations likely contributed to the increased detection in this female control mouse group; however, it may also account for the lack of significant values for the remaining cohorts. Future studies are aimed at optimizing the staining procedure with inclusion of hematoxylin staining of nuclei to help mask any non-specific red nuclear staining. In addition, analysis of images at higher magnification may aid specific stain detection. Another possible limitation was the images and analysis included only the cortex region of the kidneys and did not evaluate the juxtamedullary region. Based on histology of the tissues, there was an increased incidence of specific staining indicative of widened extra cellular matrix within the juxtamedullary region, and this area will be analyzed in future studies, with inclusion of kidney sections from additional mice in each experimental group. Lastly, the 10-week experimental duration may not be sufficient to cause significant differences among the mouse groups, and longer duration of diet and treatment exposures may be required for histological changes to be observed. Previous reports of mice on a HFD with a similar duration as the current study were also unable to find differences in picro-sirius red staining (Sanchez-Navarro et al., 2021).

Fibronectin is a major structural protein within the extracellular matrix. In kidney injury, as cells are damaged or undergo cell death due to necrosis or apoptosis, abundance of matrix

proteins increases, and this was tested to determine if SB exposure may induce fibronectin. This study found no differences in fibronectin abundance between males and females under either diet or treatment changes. Upregulation in expression of matrix proteins in response to injury or disease occurs before appreciable tissue histologic observations. In addition, the whole kidney extract preparations used for western blotting may not include proteins from the insoluble ECM fractions. Therefore, future studies are aimed at analysis of fibronectin by immunohistochemistry of kidney sections to be able to determine cellular and extracellular expression/abundance.

Superoxide dismutase (SOD-1) is an enzyme largely responsible for neutralizing superoxide, and alterations in the amount of SOD-1 in the kidney may impact the ability to resist oxidative stress. There were no significant differences noted in SOD-1 abundance in any of the cohorts. This is in contrast to prior studies which reported decreased SOD-1 abundance (Abdelhakim 2023). Future studies will analyze SOD-1 activity. Glutamyl cysteine synthetase (GCS) was analyzed because it is the first enzyme in the pathway of glutathione synthesis, a critical element for reducing oxidative radicals. This is unique compared to prior studies which have instead analyzed abundance of glutathione. Other studies analyzing GSH have reported decreased abundance following increased exposure dosages (Olofinnade 2021). This study reports a significant decrease of GCS abundance in males, which would directly reduce synthesis of GSH and is consistent with prior studies. There was no significant difference observed in female cohorts for GCS abundance. Future studies will analyze expression of GCS in additional mice in each experimental group.

## **CONCLUSIONS**

Compared to previous reports on effects of SB on kidneys, design of the current study is unique in examining the combined effects of high fat diets, known to lead to kidney injury, with SB. This was to more closely resemble the effects of SB in the setting of obesity. Furthermore, contrary to the majority of reports, the current study included both male and female mice. The addition of SB did not alter the effects of HFD on body weight in males. In addition, the promising findings of decreased GCS expression in male mice and the effects of HFD and SB on GCS will continue to be examined in additional mice in each group, due to the limited sample size in this current study. Future studies on analysis of markers of oxidative stress and analysis of specific ECM proteins will aid in defining the combined effects of HFD and SB in male and female mice.

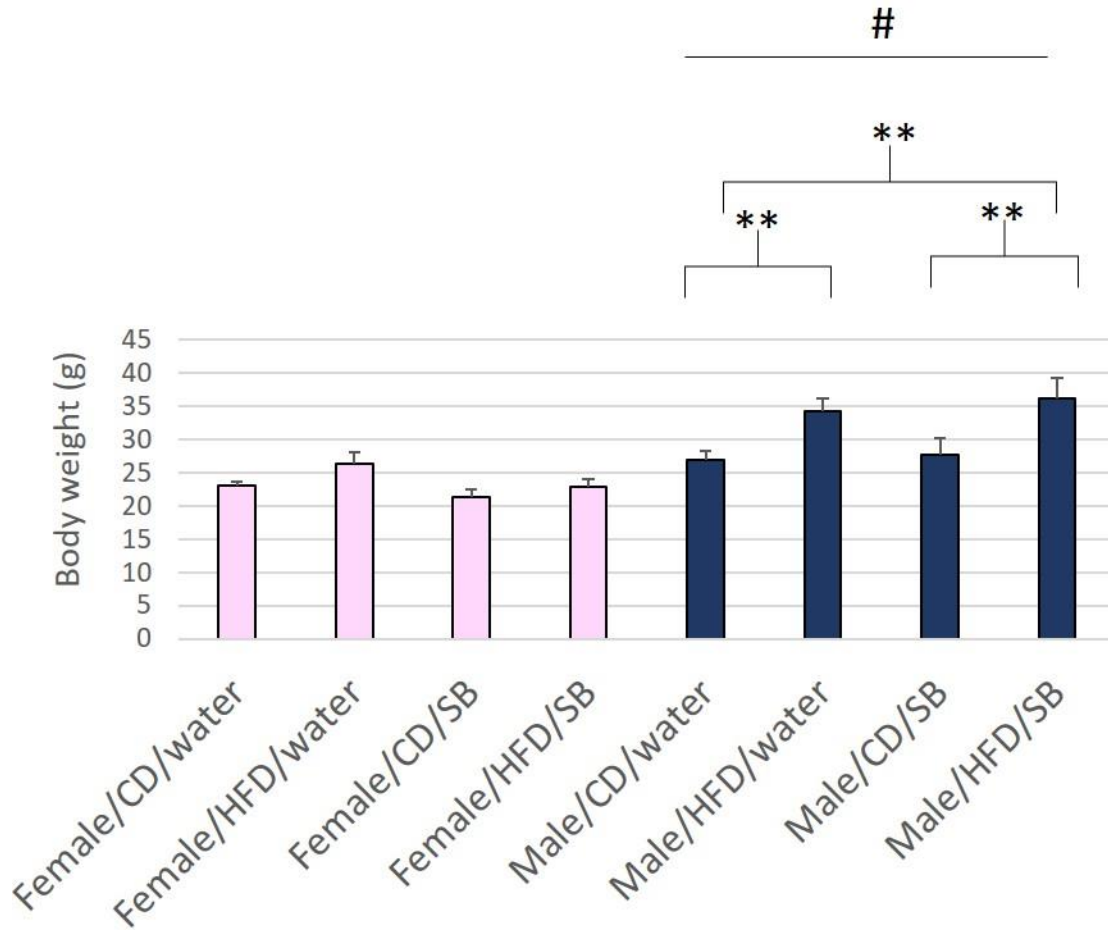


Figure 1: Effect of high fat diet and SB on body weight of female and male mice. Bars in graph represent average +/- standard deviation in each group. N=4, male/CD/SB group and female/HFD/SB group; N=5, all other mouse groups.

# Indicates a significant interaction between sex with a p-value =  $4.38 \times 10^{-14}$ , from 3-way ANOVA test. \*\* Indicates significant interaction in males between sex and diet and also sex and treatment with a p-value of less than 0.01, by Tukey test.

Tukey test indicated significant difference between male/CD/SB and male/HFD/SB, male/CD/water and male/HFD/SB, male/CD/water and male/HFD/water. SB was not additive to the effect of HFD on male bodyweight. No significant differences noted on post-hoc analysis within female groups.

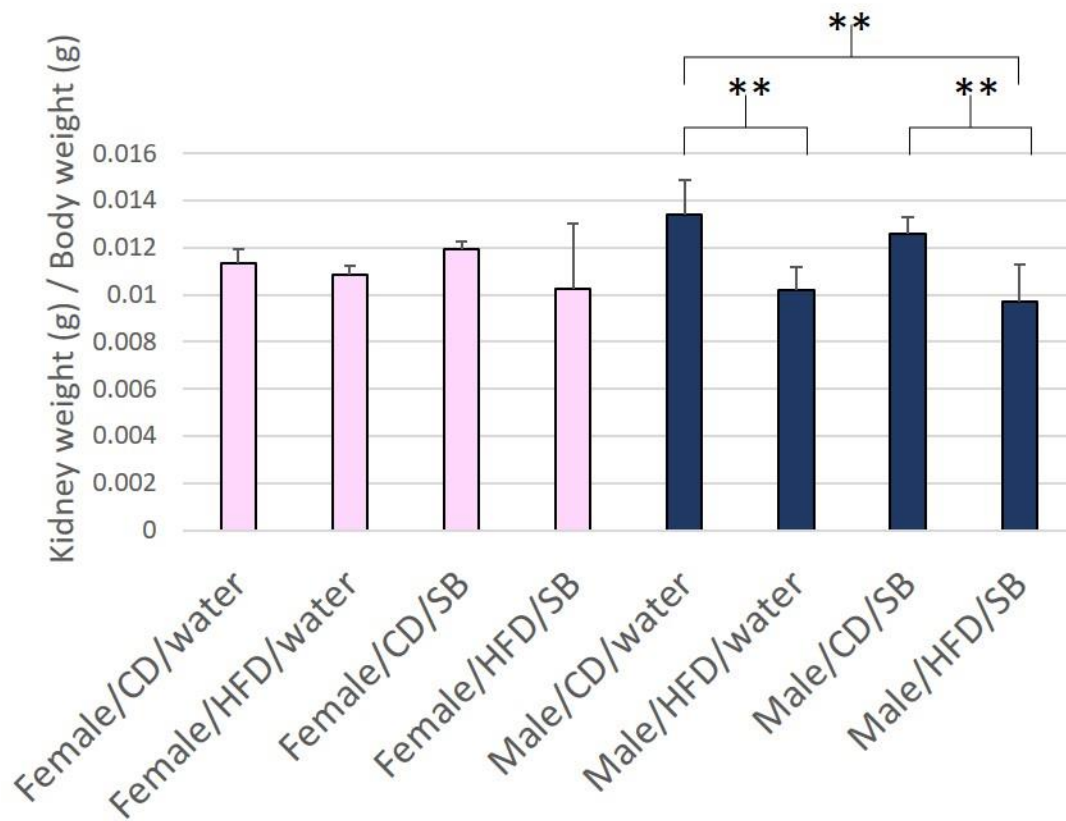


Figure 2: Effect of high fat diet and SB on kidney weight to body weight ratio in female and male mice. Bars in graph represent average +/- standard deviation in each group. N=4, male/CD/SB group and female/HFD/SB group; N=5, all other mouse groups.

\*\* Indicates significant interaction with p-value of less than 0.05.

3-way ANOVA indicated a significant interaction between sex with  $p=0.01$  and a significant interaction in males between diet and treatment. Post-hoc analysis did not reveal any significant interactions in female groups. These results show that there was no kidney hypertrophy associated with increased bodyweight gain in male mice.

## Females

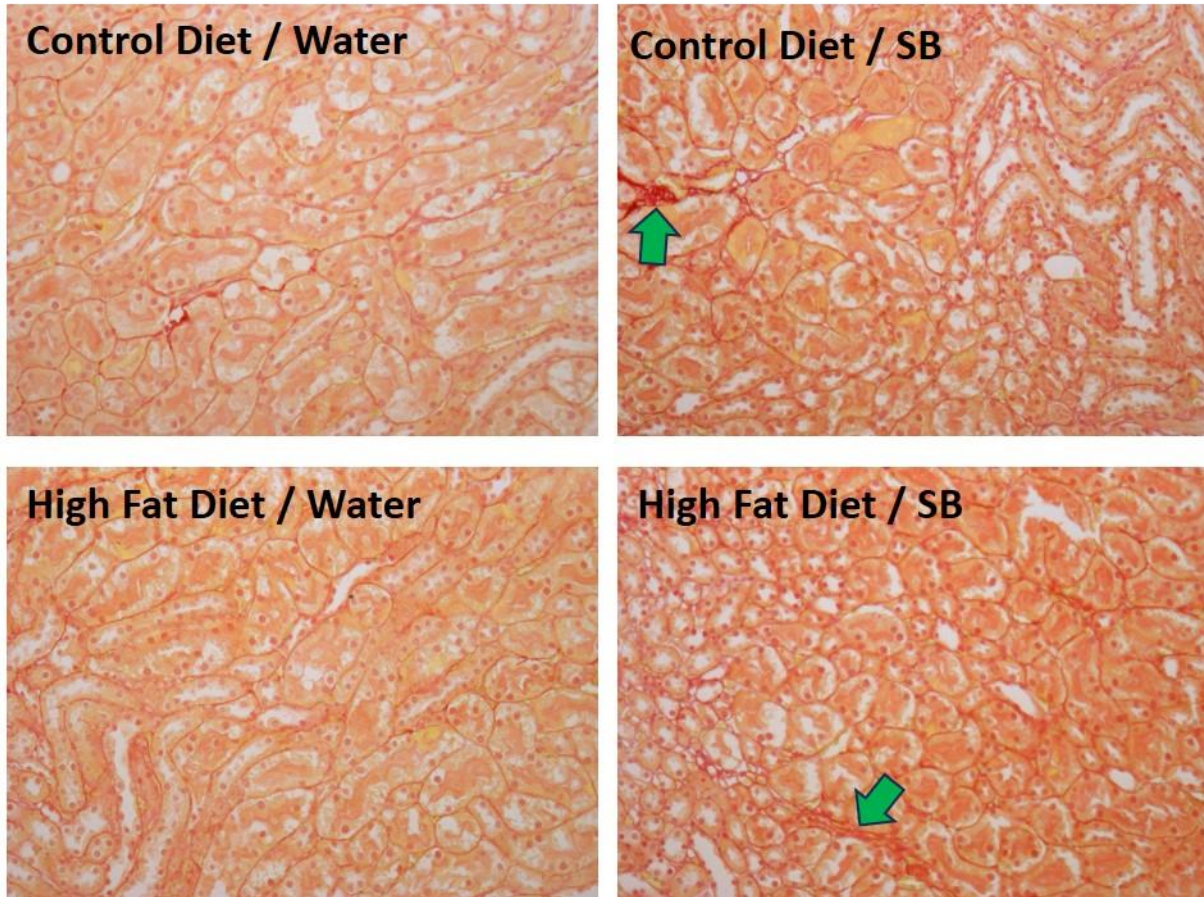


Figure 3: Picro-Sirius red staining of kidney sections in female mice. Images shown are representative of kidney cortex regions. Green arrows indicate positive staining for collagen fibers of the ECM in interstitium of kidneys. Original magnification, 40x.



Males

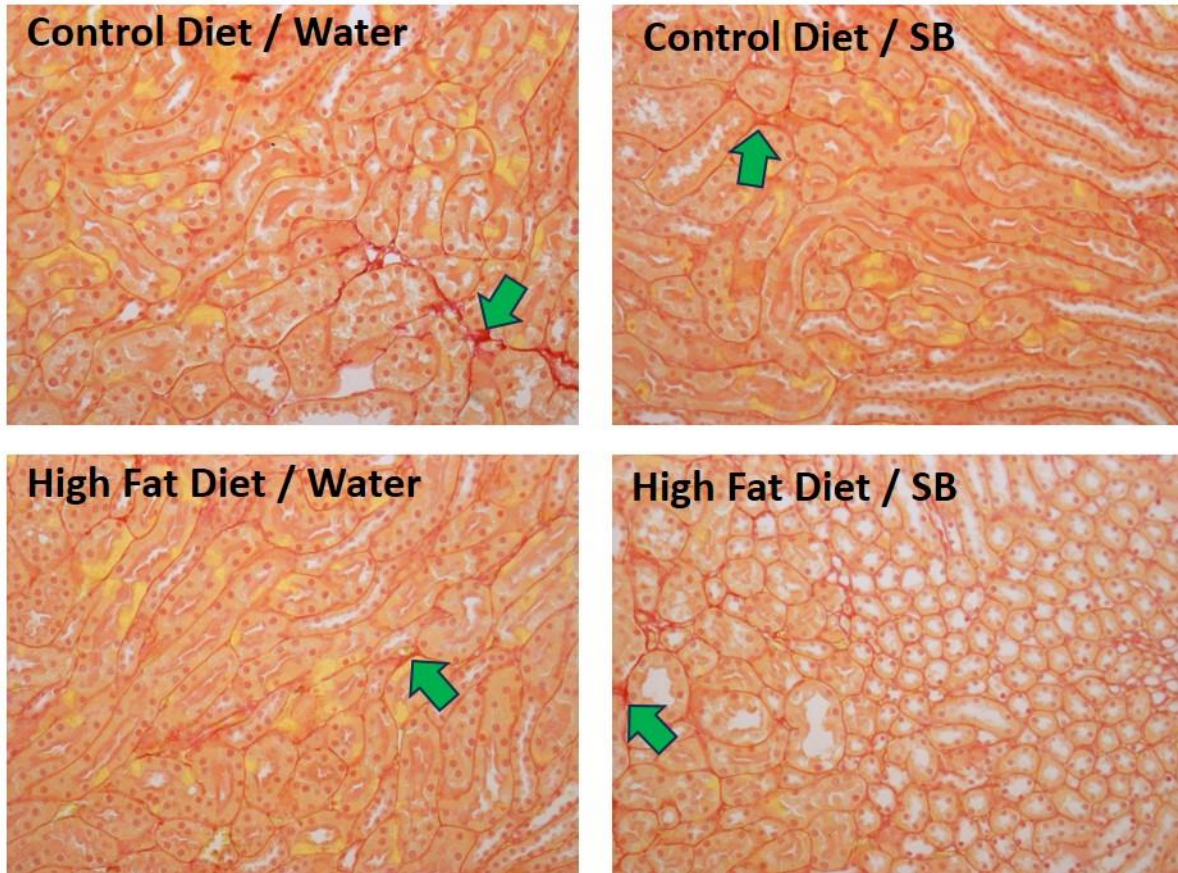


Figure 4: Picro-Sirius red staining of kidney sections in male mice. Images shown are representative of kidney cortex regions. Green arrows indicate positive staining for collagen fibers of the ECM in interstitium of kidneys. Original magnification, 40x.

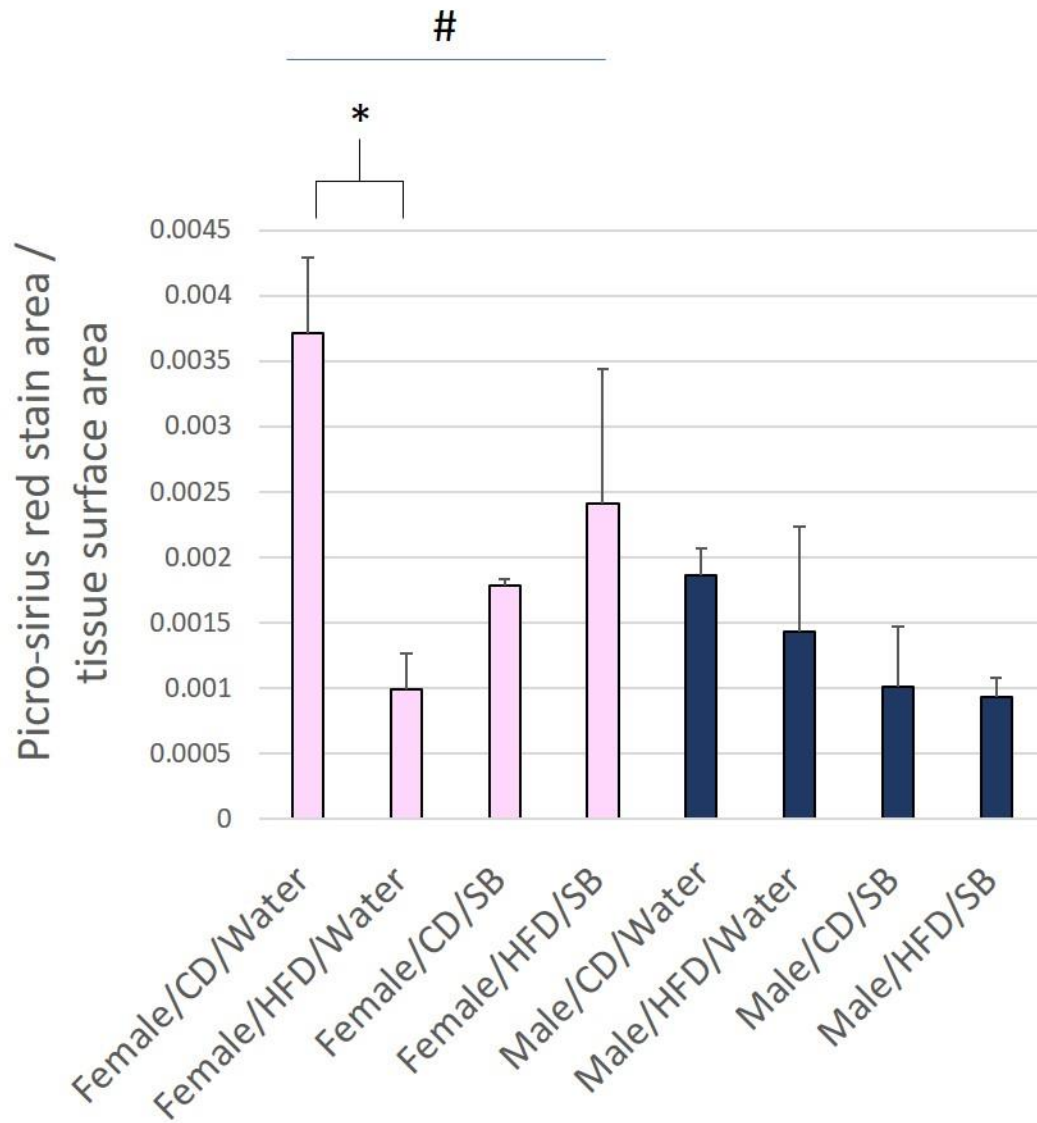


Figure 5: Analysis of picro-sirius red staining in kidney sections. Ratio of area of Picro-Sirius red stain detected to total surface area of cortex tissue analyzed. Bars in graph represent average +/- SEM for each group.

# Indicates p-value < 0.05, females vs males, 3-way ANOVA test. \* Indicates p-value < 0.05, Tukey test. No significant differences in male groups revealed by Tukey test. N=3/group.



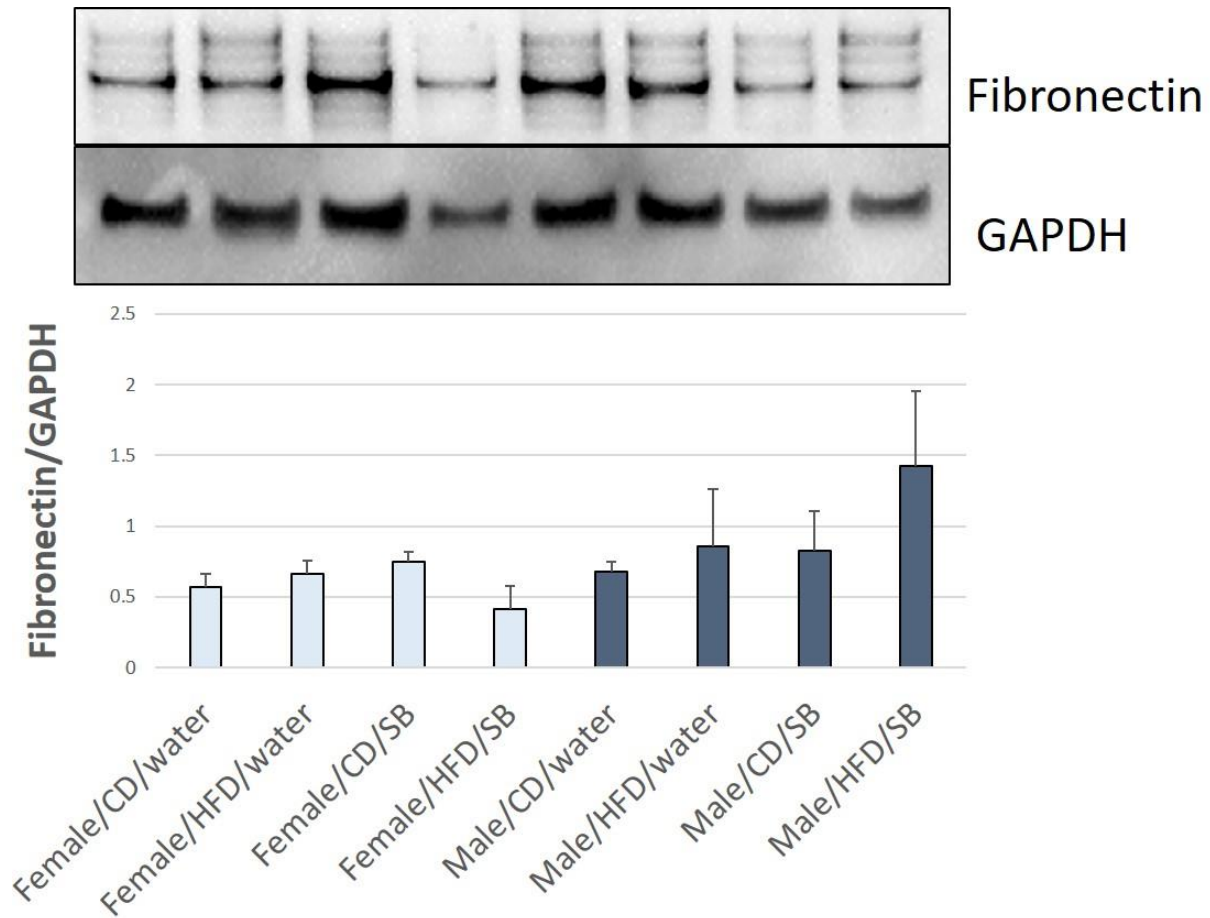


Figure 6: Effect of high fat diet and SB on fibronectin protein abundance in kidneys from female and male kidneys. Western blot of fibronectin and GAPDH (lane protein loading control) are shown. Western blot lanes are aligned with and lane identification indicated by the bar graph below the blots. Bars in graph represents ratio of fibronectin protein band densitometry to that of GAPDH in each lane, to normalize for protein loading in each lane. Fibronectin was not different between any experimental groups in males or females. N=3/mouse group.

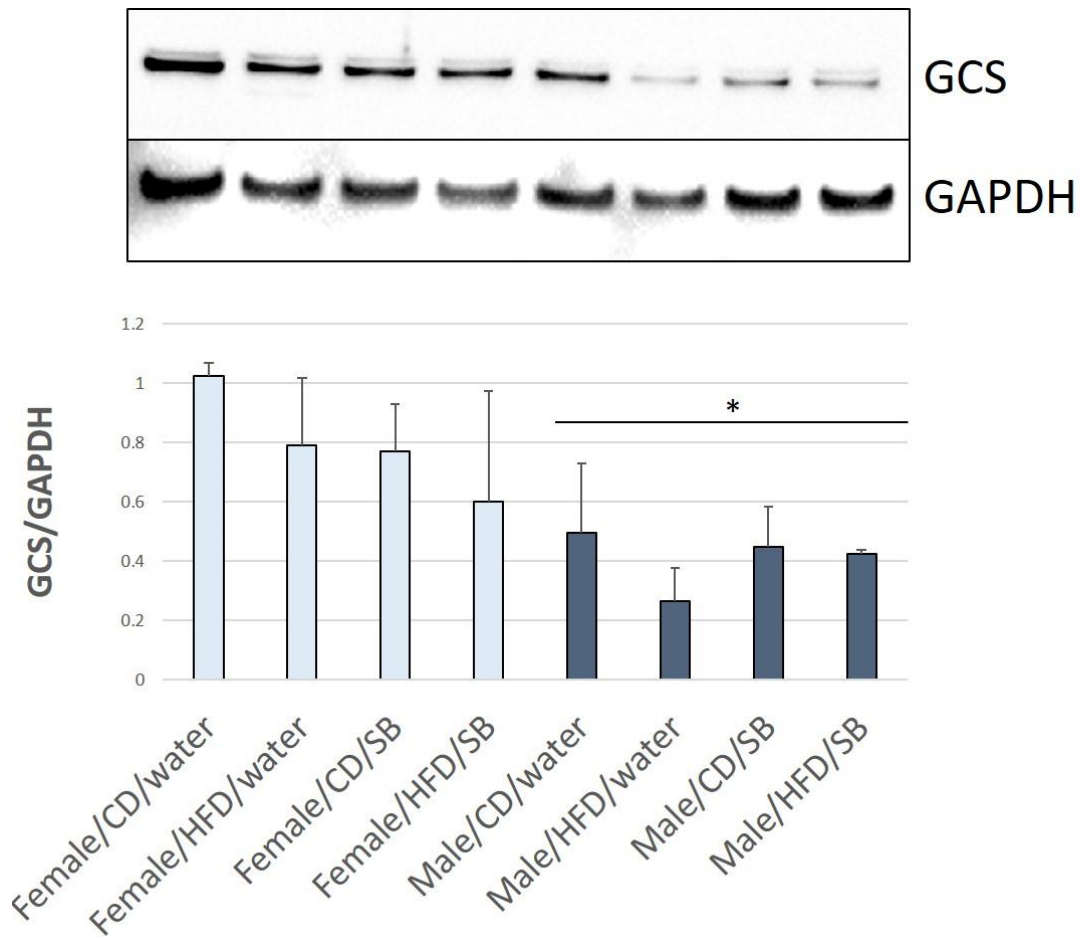


Figure 7: Effect of high fat diet and SB on GCS protein abundance in kidneys from female and male kidneys. Western blot of GCS and GAPDH (lane protein loading control) are shown. Western blot lanes are aligned with lane identification indicated by the bar graph below the blots. Bars in graph represents ratio of GCS protein band densitometry to that of GAPDH in each lane, to normalize for protein loading in each lane.  
 \*Indicates p-value < 0.05 male vs female. No significant differences in experimental groups in either male or female mice. N=3/mouse group.

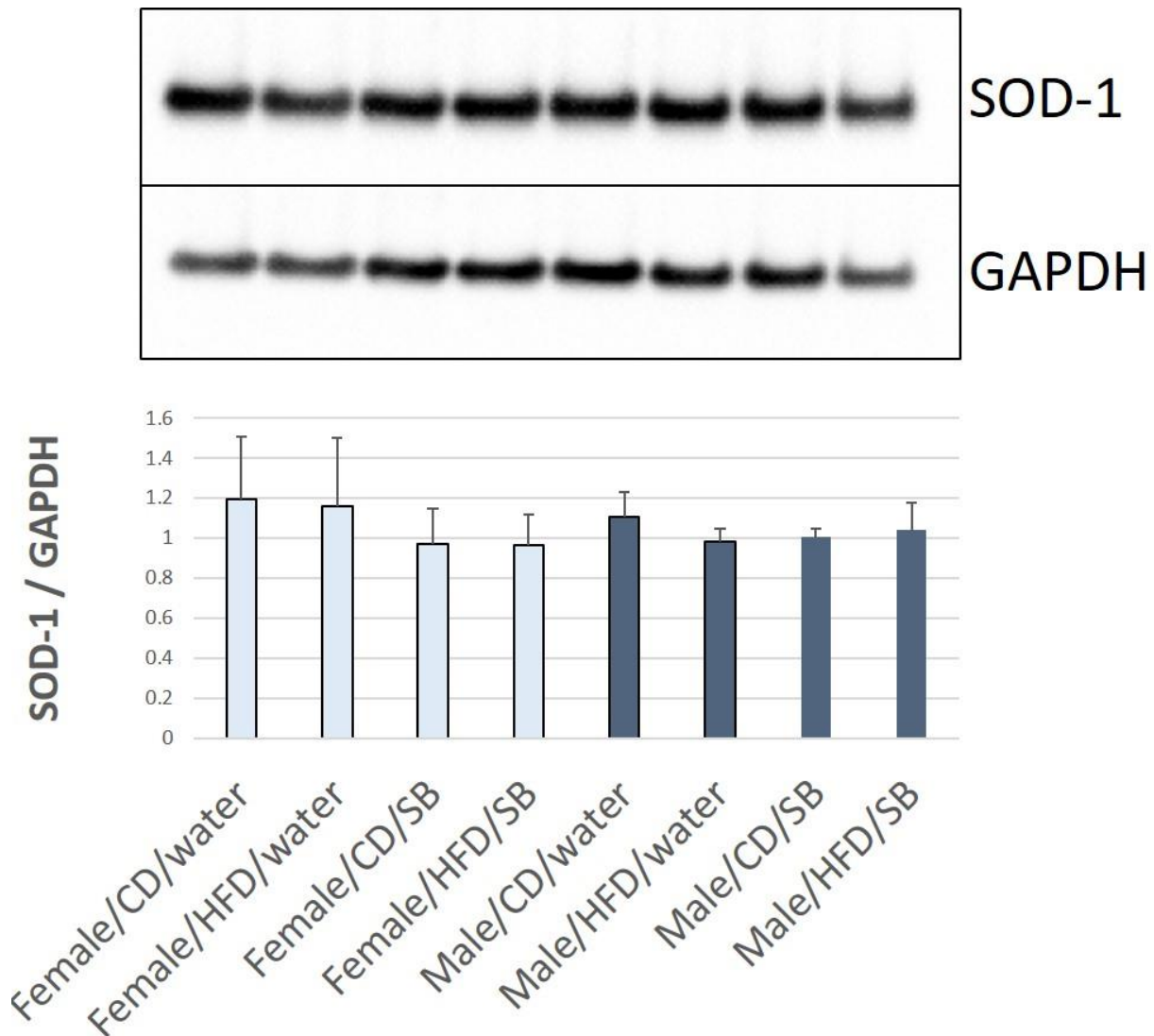


Figure 8: Effect of high fat diet and SB on SOD-1 protein abundance in kidneys from female and male kidneys. Western blot of SOD-1 and GAPDH (lane protein loading control) are shown. Western blot lanes are aligned with- and lane identification indicated by the bar graph below the blots. Bars in graph represents ratio of SOD-1 protein band densitometry to that of GAPDH in each lane, to normalize for protein loading in each lane. No significant differences found between any of the experimental mouse groups. N=3/mouse group.

## Acknowledgements

I thank my mentor, Dr. Michelle Barati, Ph.D. of the Division of Nephrology, for her constant guidance and support during my time as an undergraduate researcher. Dr. Loretta Jophlin, M.D., Ph.D. of the Department of Gastroenterology & Digestive and Liver Health, for providing the mouse kidney samples from her studies. And Dr. Adam Gaweda, Ph.D. of the Division of Nephrology for providing assistance and guidance with statistical analysis.

## References

Abd-Elhakim, Y. M., Behairy, A., Hashem, M. M., Abo-EL-Sooud, K., El-Metwally, A. E., Hassan, B. A., & Ali, H. A. (2023). Toll-like receptors and nuclear factor kappa B signaling pathway involvement in hepatorenal oxidative damage induced by some food preservatives in rats. *Scientific Reports*, *13*(1). <https://doi.org/10.1038/s41598-023-32887-9>

Badenhorst CP, Erasmus E, van der Sluis R, Nortje C, van Dijk AA. A new perspective on the importance of glycine conjugation in the metabolism of aromatic acids. *Drug Metab Rev*. 2014 Aug;*46*(3):343-61. doi: 10.3109/03602532.2014.908903. Epub 2014 Apr 22. PMID: 24754494.

Bülow RD, Boor P. Extracellular Matrix in Kidney Fibrosis: More Than Just a Scaffold. *J Histochem Cytochem*. 2019 Sep;*67*(9):643-661. doi: 10.1369/0022155419849388. Epub 2019 May 22. PMID: 31116062; PMCID: PMC6713975.

Castañeda-Bueno M, Ellison DH, Gamba G. Molecular mechanisms for the modulation of blood pressure and potassium homeostasis by the distal convoluted tubule. *EMBO Mol Med*. 2022 Feb 7;*14*(2):e14273. doi: 10.15252/emmm.202114273. Epub 2021 Dec 20. PMID: 34927382; PMCID: PMC8819348.

CFR—Code of Federal Regulations Title 21. [(accessed on 1 February 2024)]; <https://www.accessdata.fda.gov/scripts/cdrh/cfdocs/cfcfr/cfrsearch.cfm?fr=184.1733>

Centers for Disease Control and Prevention. (n.d.). *Achievements in public health, 1900-1999: Safer and healthier foods*. Centers for Disease Control and Prevention. <https://www.cdc.gov/mmwr/preview/mmwrhtml/mm4840a1.htm>

Chen TK, Knicely DH, Grams ME. Chronic Kidney Disease Diagnosis and Management: A Review. *JAMA*. 2019 Oct 1;*322*(13):1294-1304. doi: 10.1001/jama.2019.14745. PMID: 31573641; PMCID: PMC7015670.

Chen Y, Ma Y, Ma W. Pharmacokinetics and bioavailability of cinnamic acid after oral administration of *Ramulus Cinnamomi* in rats. *Eur J Drug Metab Pharmacokinet*. 2009 Jan-Mar;34(1):51-6. doi: 10.1007/BF03191384. PMID: 19462929.

Dantzler WH, Pannabecker TL, Layton AT, Layton HE. Urine concentrating mechanism in the inner medulla of the mammalian kidney: role of three-dimensional architecture. *Acta Physiol (Oxf)*. 2011 Jul;202(3):361-78. doi: 10.1111/j.1748-1716.2010.02214.x. Epub 2010 Dec 7. PMID: 21054810; PMCID: PMC3807677.

Davidson, P.M., Sofos, J.N., & Branen, A.L. (Eds.). (2005). *Antimicrobials in Food* (3rd ed.). CRC Press. <https://doi.org/10.1201/9781420028737>

Declèves AE, Zolkipli Z, Satriano J, Wang L, Nakayama T, Rogac M, Le TP, Nortier JL, Farquhar MG, Naviaux RK, Sharma K. Regulation of lipid accumulation by AMP-activated kinase [corrected] in high fat diet-induced kidney injury. *Kidney Int*. 2014 Mar;85(3):611-23. doi: 10.1038/ki.2013.462. Epub 2013 Dec 4. Erratum in: *Kidney Int*. 2014 Jun;85(6):1474. Erratum in: *Kidney Int*. 2017 Sep;92(3):769. PMID: 24304883; PMCID: PMC4244908.

Deji N, Kume S, Araki S, Soumura M, Sugimoto T, Isshiki K, Chin-Kanasaki M, Sakaguchi M, Koya D, Haneda M, Kashiwagi A, Uzu T. Structural and functional changes in the kidneys of high-fat diet-induced obese mice. *Am J Physiol Renal Physiol*. 2009 Jan;296(1):F118-26. doi: 0.1152/ajprenal.00110.2008. Epub 2008 Oct 29. PMID: 18971213.

*Food Safety and Inspection Service*. Molds on Food: Are They Dangerous? | Food Safety and Inspection Service. (n.d.). <https://www.fsis.usda.gov/food-safety/safe-food-handling-and-preparation/food-safety-basics/molds-food-are-they-dangerous>

Fujitani, T. 1993 . Short-term effect of sodium benzoate in F344 rats and B6C3F1 mice. *Toxicol. Lett.(Amst)*69:171–179.

Gardner LK, Lawrence GD. 1993. Benzene production from decarboxylation of benzoic acid in the presence of ascorbic acid and a transition metal catalyst. *J Agric Food Chem* 40: 693–5

Ha S, Yang Y, Kim BM, Kim J, Son M, Kim D, Yu HS, Im DS, Chung HY, Chung KW. Activation of PAR2 promotes high-fat diet-induced renal injury by inducing oxidative stress and inflammation. *Biochim Biophys Acta Mol Basis Dis*. 2022 Oct 1;1868(10):166474. doi: 10.1016/j.bbadis.2022.166474. Epub 2022 Jun 27. PMID: 35772632.

Horita, S., Nakamura, M., Suzuki, M., Satoh, N., Suzuki, A., Homma, Y., & Nangaku, M. (2017). The role of renal proximal tubule transport in the regulation of Blood Pressure. *Kidney Research and Clinical Practice*, 36(1), 12–21. <https://doi.org/10.23876/j.krcp.2017.36.1.12>

Ikarashi Y, Uchino T, Nishimura T. [Analysis of preservatives used in cosmetic products: salicylic acid, sodium benzoate, sodium dehydroacetate, potassium sorbate, phenoxyethanol, and parabens]. *Kokuritsu Iyakuin Shokuhin Eisei Kenkyusho Hokoku*. 2010;(128):85-90. Japanese. PMID: 21381401.

Informatics, Inc. 1972 . GRAS(generally recognized as safe) foodingredients: Benzoic Acid and Sodium Benzoate. NTIS Report No. PB-221-208.

Jackson LS. Chemical food safety issues in the United States: past, present, and future. *J Agric Food Chem.* 2009 Sep 23;57(18):8161-70. doi: 10.1021/jf900628u. PMID: 19719131.

Juul, F., Parekh, N., Martinez-Steele, E., Monteiro, C. A., & Chang, V. W. (2022). Ultra-processed food consumption among US adults from 2001 to 2018. *The American Journal of Clinical Nutrition*, 115(1), 211–221. <https://doi.org/10.1093/ajcn/nqab305>

Kambham N, Markowitz GS, Valeri AM, Lin J, D'Agati VD. Obesity-related glomerulopathy: an emerging epidemic. *Kidney Int.* 2001 Apr;59(4):1498-509. doi: 10.1046/j.1523-1755.2001.0590041498.x. PMID: 11260414.

Kubota K, Ishizaki T. Dose-dependent pharmacokinetics of benzoic acid following oral administration of sodium benzoate to humans. *Eur J Clin Pharmacol.* 1991;41(4):363-8. doi: 10.1007/BF00314969. PMID: 1804654.

Lane HY, Lin CH, Green MF, Hellemann G, Huang CC, Chen PW, Tun R, Chang YC, Tsai GE. Add-on treatment of benzoate for schizophrenia: a randomized, double-blind, placebo-controlled trial of D-amino acid oxidase inhibitor. *JAMA Psychiatry.* 2013 Dec;70(12):1267-75. doi: 10.1001/jamapsychiatry.2013.2159. PMID: 24089054.

Lennerz, B. S., Vafai, S. B., Delaney, N. F., Clish, C. B., Deik, A. A., Pierce, K. A., Ludwig, D. S., & Mootha, V. K. (2015). Effects of sodium benzoate, a widely used food preservative, on glucose homeostasis and metabolic profiles in humans. *Molecular Genetics and Metabolism*, 114(1), 73–79. <https://doi.org/10.1016/j.ymgme.2014.11.010>

Lin, C.-H., Chen, P.-K., Chang, Y.-C., Chuo, L.-J., Chen, Y.-S., Tsai, G. E., & Lane, H.-Y. (2014a). Benzoate, a D-amino acid oxidase inhibitor, for the treatment of early-phase alzheimer disease: A randomized, double-blind, placebo-controlled trial. *Biological Psychiatry*, 75(9), 678–685. <https://doi.org/10.1016/j.biopsych.2013.08.010>

MacKay MB, Kravtsenyuk M, Thomas R, Mitchell ND, Dursun SM, Baker GB. D-Serine: Potential Therapeutic Agent and/or Biomarker in Schizophrenia and Depression? *Front Psychiatry.* 2019 Feb 6;10:25. doi: 10.3389/fpsy.2019.00025. PMID: 30787885; PMCID: PMC6372501. Matsuura A, Fujita Y, Iyo M, Hashimoto K. Effects of sodium benzoate on pre-pulse inhibition deficits and hyperlocomotion in mice after administration of phencyclidine. *Acta Neuropsychiatrica.* 2015;27(3):159-167. doi:10.1017/neu.2015.1

McNeal T. P., Nyman P. J., Diachenko G. W., Hollifield H. C. Survey of benzene in foods by using headspace concentration techniques and capillary gas chromatography. *Journal of AOAC International.* 1993;76(6):1213–1219

Merchant ML, Barati MT, Caster DJ, Hata JL, Hobeika L, Coventry S, Brier ME, Wilkey DW, Li M, Rood IM, Deegens JK, Wetzels JF, Larsen CP, Troost JP, Hodgins JB, Mariani LH, Kretzler M, Klein JB, McLeish KR. Proteomic Analysis Identifies Distinct Glomerular

Extracellular Matrix in Collapsing Focal Segmental Glomerulosclerosis. *J Am Soc Nephrol*. 2020 Aug;31(8):1883-1904. PMID: 32561683; PMCID: PMC7460901.

Mineo H, Ohdate T, Fukumura K, Katayama T, Onaga T, Kato S, Yanaihara N. Effects of benzoic acid and its analogues on insulin and glucagon secretion in sheep. *Eur J Pharmacol*. 1995 Jul 4;280(2):149-54. doi: 10.1016/0014-2999(95)00192-n. PMID: 7589179.

Misel ML, Gish RG, Patton H, Mendler M. Sodium benzoate for treatment of hepatic encephalopathy. *Gastroenterol Hepatol (N Y)*. 2013 Apr;9(4):219-27. PMID: 24711766; PMCID: PMC3977640.

Nair B. Final report on the safety assessment of Benzyl Alcohol, Benzoic Acid, and Sodium Benzoate. *Int J Toxicol*. 2001;20 Suppl 3:23-50. doi: 10.1080/10915810152630729. PMID: 11766131.

Nicholas Lawrance, Sophie Gaikwad, Catherine Holden, CD01 Sodium benzoate: an important allergen to patch test to — is 5% in petrolatum too irritant?, *British Journal of Dermatology*, Volume 188, Issue Supplement\_4, June 2023, ljad113.200, <https://doi.org/10.1093/bjd/ljad113.200>

Nie X, Li C, Hu S, Xue F, Kang YJ, Zhang W. An appropriate loading control for western blot analysis in animal models of myocardial ischemic infarction. *Biochem Biophys Res*. 2017 Sep 12;12:108-113. PMID: 28955798; PMCID: PMC5613232.

Odeyemi OA, Alegbeleye OO, Strateva M, Stratev D. Understanding spoilage microbial community and spoilage mechanisms in foods of animal origin. *Compr Rev Food Sci Food Saf*. 2020 Mar;19(2):311-331. doi: 10.1111/1541-4337.12526. Epub 2020 Jan 20. PMID: 33325162.

Olofinnade Anthony Tope, Adejoke Yetunde Onaolapo, Olakunle James Onaolapo, Olugbenga Adekunle Olowe, The potential toxicity of food-added sodium benzoate in mice is concentration-dependent, *Toxicology Research*, Volume 10, Issue 3, May 2021, Pages 561–569, <https://doi.org/10.1093/toxres/tfab024>

Oshima Y, Wakino S, Kanda T, Tajima T, Itoh T, Uchiyama K, Yoshimoto K, Sasabe J, Yasui M, Itoh H. Sodium benzoate attenuates 2,8-dihydroxyadenine nephropathy by inhibiting monocyte/macrophage TNF- $\alpha$  expression. *Sci Rep*. 2023 Feb 27;13(1):3331.

Piper JD, Piper PW. Benzoate and sorbate salts: a systematic review of the potential hazards of these invaluable preservatives and the expanding spectrum of clinical uses for sodium benzoate. *Comprehensive Reviews in Food Science and Food Safety*. 2017;16:868-80

Pongsavee M. Effect of sodium benzoate preservative on micronucleus induction, chromosome break, and Ala40Thr superoxide dismutase gene mutation in lymphocytes. *Biomed Res Int*. 2015;2015:103512. doi: 10.1155/2015/103512. Epub 2015 Feb 17. PMID: 25785261; PMCID: PMC4346689.

Potential therapeutic agent and/or biomarker in schizophrenia and depression? *Frontiers in Psychiatry*, 10. <https://doi.org/10.3389/fpsy.2019.00025>

Ranieri M, Di Mise A, Tamma G, Valenti G. Vasopressin-aquaporin-2 pathway: recent advances in understanding water balance disorders. *F1000Res*. 2019 Feb 4;8:F1000 Faculty Rev-149. doi: 10.12688/f1000research.16654.1. PMID: 30800291; PMCID: PMC6364380.

Sánchez-Navarro, A., Martínez-Rojas, M. Á., Caldiño-Bohn, R. I., Pérez-Villalva, R., Zambrano, E., Castro-Rodríguez, D. C., & Bobadilla, N. A. (2021). Early triggers of moderately high-fat diet-induced kidney damage. *Physiological Reports*, 9(14). <https://doi.org/10.14814/phy2.14937>

Schaubschläger W.W., Becker W.M., Schade U., Zabel P., Schlaak M. Release of Mediators from Human Gastric Mucosa and Blood in Adverse Reactions to Benzoate. *Int. Arch. Allergy Appl. Immunol.* 1991;96:97–101

Shah SV, Walker PD. Evidence suggesting a role for hydroxyl radical in glycerol-induced acute renal failure. *Am J Physiol.* 1988 Sep;255(3 Pt 2):F438-43.

Shah SV. Evidence suggesting a role for hydroxyl radical in passive Heymann nephritis in rats. *Am J Physiol.* 1988 Mar;254(3 Pt 2):F337-44.

Shahmohammadi, M., Javadi, M., & Nassiri-Asl, M. (2016). An overview on the effects of sodium benzoate as a preservative in food products. *Biotechnology and Health Sciences*, 3(3), 7-11.

Sim G. A., Robertson J. M., Goodwin T. H. The crystal and molecular structure of benzoic acid. *Acta Crystallographica*. 1955;8(3):157–164. doi: 10.1107/S0365110X55000601.

Spustová V, Dzúrik R, Geryková M. Hippurate participation in the inhibition of glucose utilization in renal failure. *Czech Med.* 1987;10(2):79–89

Stierman, Bryan et al. (2021). National Health and Nutrition Examination Survey 2017–March 2020 Prepandemic Data Files Development of Files and Prevalence Estimates for Selected Health Outcomes. (158).

Sun Y, Ge X, Li X, He J, Wei X, Du J, Sun J, Li X, Xun Z, Liu W, Zhang H, Wang ZY, Li YC. High-fat diet promotes renal injury by inducing oxidative stress and mitochondrial dysfunction. *Cell Death Dis.* 2020 Oct 24;11(10):914. doi: 10.1038/s41419-020-03122-4. PMID: 33099578; PMCID: PMC7585574.

Sushma S, Dasarathy S, Tandon RK, Jain S, Gupta S, Bhist MS. Sodium benzoate in the treatment of acute hepatic encephalopathy: a double-blind randomized trial. *Hepatology*. 1992 Jul;16(1):138-44. doi: 10.1002/hep.1840160123. PMID: 1618465.

Tfouni SA, Toledo MC. Estimates of the mean per capita daily intake of benzoic and sorbic acids in Brazil. *Food Addit Contam.* 2002 Jul;19(7):647-54. doi: 10.1080/02652030210125119. PMID: 12113659.



Traynor J, Mactier R, Geddes CC, Fox JG. How to measure renal function in clinical practice. *BMJ*. 2006 Oct 7;333(7571):733-7. doi: 10.1136/bmj.38975.390370.7C. PMID: 17023465; PMCID: PMC1592388.

Thakur V, Walker PD, Shah SV. Evidence suggesting a role for hydroxyl radical in puromycin aminonucleoside-induced proteinuria. *Kidney Int*. 1988 Oct;34(4):494-9. doi: 10.1038/ki.1988.208. PMID: 2848972.

United States Renal Data System. 2023 *USRDS Annual Data Report: Epidemiology of kidney disease in the United States*. National Institutes of Health, National Institute of Diabetes and Digestive and Kidney Diseases, Bethesda, MD, 2023.

U.S. Department of Health and Human Services. (n.d.). *What is alzheimer's disease?* National Institute on Aging. <https://www.nia.nih.gov/health/alzheimers-and-dementia/what-alzheimers-disease>

de Vries A, Alexander B, Quamo Y. Studies on Amino Acid Metabolism. Iii. Plasma Glycine Concentration and Hippuric Acid Formation Following the Ingestion of Benzoate. *J Clin Invest*. 1948;27(5):665–8).

Wang M, Wang Z, Chen Y, Dong Y. Kidney Damage Caused by Obesity and Its Feasible Treatment Drugs. *Int J Mol Sci*. 2022 Jan 11;23(2):747. doi: 10.3390/ijms23020747. PMID: 35054932; PMCID: PMC8775419.

Walczak-Nowicka, Ł. J., & Herbet, M. (2022). Sodium benzoate—harmfulness and potential use in therapies for disorders related to the nervous system: A Review. *Nutrients*, 14(7), 1497. <https://doi.org/10.3390/nu14071497>

Walker PD, Shah SV. Evidence suggesting a role for hydroxyl radical in gentamicin-induced acute renal failure in rats. *J Clin Invest*. 1988 Feb;81(2):334-41.

Widmaier, E. P., Raff, H., Strang, K. T., & Vander, A. J. (2023a). *Vander's human physiology: The mechanisms of body function*. McGraw Hill LLC.

Williams RE, Lock EA. Sodium benzoate attenuates D-serine induced nephrotoxicity in the rat. *Toxicology*. 2005 Feb 1;207(1):35-48. doi: 10.1016/j.tox.2004.08.008. PMID: 15590120.

World Health Organization. (n.d.). World Health Organization. <https://apps.who.int/food-additives-contaminants-jecfa-database/Home/Chemical/1098>

Zeghib K, Boutlelis DA. Food Additive (Sodium benzoate)-induced Damage on Renal Function and Glomerular Cells in Rats; Modulating Effect of Aqueous Extract of *Atriplex halimus* L. *Iran J Pharm Res*. 2021 Winter;20(1):296-306. doi: 10.22037/ijpr.2020.111634.13272. PMID: 34400959; PMCID: PMC8170748.

